Journal of Materials Chemistry A

Accepted Manuscript

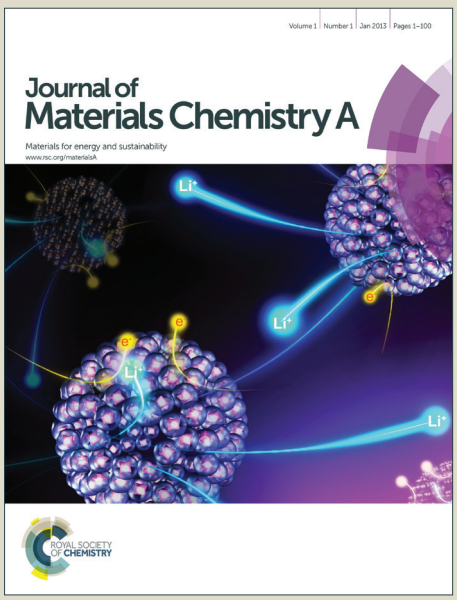

ROYAL SOCIETY OF CHEMISTRY

www.rsc.org/materialsA

Journal Name Journal of Materials Chemistry A Dynamic Article Links ►

Cite this: DOI: 10.1039/c0xx00000x

www.rsc.org/xxxxxx

ARTICLE TYPE

Amine-functionalized Metal-Organic Frameworks for transesterification of triglycerides

Jinzhu Chen,*[a] Ruliang Liu,[a,c] Hui Gao,[a,b] Limin Chen[b] and Daiqi Ye[b]

Received (in XXX, XXX) Xth XXXXXXXXX 20XX, Accepted Xth XXXXXXXXX 20XX

DOI: 10.1039/b000000x

For the application purpose of functionalized Metal-Organic Frameworks (MOFs) as solid base, amine-functionalized MOF materials are achieved by i) dative modification of unsaturated metal sites located at the secondary building units of MOFs with diamine, and ii) covalent modification of the amine-tagged organic linkers within the MOF by alkylation with 2-dimethylaminoethyl chloride. The resulting amine-functionalized MOFs exhibit excellent results in the liquid phase transesterification of triglycerides and methanol with the triglyceride conversions exceeding 99%, which are important model reactions for production of biodiesel. The relationship between the catalytic activity towards transesterification and basicity of amine-functionalized MOFs reveals a linear correspondence in term of turnover frequency and the basic site density. The basicity of MOFs and reaction parameters are shown to significantly affect catalytic performance. Kinetics studies reveal that the reaction follows first-order kinetics with the calculated activation energy of 48.2 kJ mol^{-1}. The research opens a new perspective on postsynthetic modification of MOFs and more generally on the rational design of MOF-derived solid base catalysts.

1 Introduction

Transesterification is an important transformation both in industry for biodiesel production and in laboratories for organic synthesis, which can be accomplished by acid or base catalysis.[1,2] Especially base catalysis has been deemed to be an effective method for transesterification when compared with acid catalysis.[2] In spite of continuous efforts to explore efficient and recyclable solid base catalysts such as alkali or alkaline earth oxides, supported alkali metals, basic zeolites, clay minerals, and amino-supported compounds, the development of new and green processes for solid base catalyst remains a great challenge.[3]

Owing to their versatility, Metal-Organic Frameworks (MOFs), a class of crystalline micro-mesoporous hybrid materials, have recently obtained considerable attention in heterogeneous catalysis.[4] Previously, bifunctional acid-metal catalysts containing ruthenium and polyoxometalates as active species with a MOF as support and encapsulation matrix, respectively, were synthesized by us to achieve one-pot conversion of cellobiose and cellulose into sorbitol.[5] In the MOF-derived solid base catalysis, MOFs possess three main assets: 1) a porous network which can promote adsorption and diffusion of substrate molecules such as triglycerides, 2) a degree of basicity which can be precisely tuned by postsynthetic modification (PSM), and 3) a PSM which can be achieved on an organic ligand component in MOF by employing a variety of organic transformations.

MOFs are typically prepared by a self-assembly of metal ions or clusters and polytopic bridging ligands under traditional solvothermal conditions.[6] Theoretically, the basicity of the materials can dramatically be affected by nitrogen-donor ligands, such as pyridine, pyrazine, imidazole, and tetrazole, used for incorporation with metal ions.[7] However, due to competitive coordination of these Lewis basic nitrogen sites with metal ions or clusters, directly synthesized nitrogen-rich MOFs generally present relatively low basicity. Current research on these MOFs is mainly focused on adsorption-based CO_2 separation;[8] and their further application as effective solid base is still a great challenge.[9]

In this study, amine-functionalized MOFs were achieved by two different chemical approaches: 1) dative modification of unsaturated metal sites located at the secondary building units (SBUs) of MOFs, and 2) covalent modification of the organic linkers within the MOF. The prepared amine-functionalized MOFs show excellent performance as efficient solid base catalysis toward the transesterification of triglycerides with methanol (Scheme 1a). Moreover, the relationship between the catalytic activity in term of turnover frequency (TOF) and basicity of amine-functionalized MOFs reveals a linear correspondence in transesterification.

2 Experimental

2.1 MOF-5, IRMOF-10 and MIL-53(Al)-NH_2

MOF-5,[11a] IRMOF-10[10] and MIL-53(Al)-NH_2[19b] were prepared according to literature method. (See the Supporting Information for details).

2.2 Dative PSM of MOF-5 and IRMOF-10

In a typical procedure, MOF-5 (768 mg, 1 mmol), dehydrated at 150 °C for 12 h, was suspended in anhydrous toluene (30 mL).

To this suspension, ED (360 mg, 6 mmol) was added [in the case of MOF-5-DMAP preparation, DMAP (726 mg, 6 mmol) was added], the mixture was stirred with heating to reflux for 24 h under nitrogen to give MOF-5-ED. The remaining solid was filtered off, washed with anhydrous toluene, and further treated at 100 °C *in vacuo* (1×10^{-7} Torr) for 24 h to remove any physisorbed ED. IRMOF-10-ED and IRMOF-10-DMAP were prepared following the reaction conditions similar to that of MOF-5-ED and MOF-5-DMAP, respectively.

2.3 Covalent PSM of MIL-53(Al)-NH_2

In a typical procedure, a suspension of MIL-53(Al)-NH_2 (630 mg, 3 mmol) in water (10 mL) is treated with 2-dimethylaminoethyl chloride hydrochloride (144 mg, 10 mmol) and potassium carbonate (276 mg, 20 mmol) at 80 °C for 2 days under nitrogen. The obtained solid MIL-53(Al)-NH-NMe_2 was filtered off, washed with water, and dried at 90 °C under vacuum for 24 h.

2.4 Transesterification of triacetin with methanol

Transesterification reactions were performed in a thermostatted Ace Pressure Tube. The reactants were always loaded into the reactor at ambient temperature. Glyceryl triacetate (181 mg, 0.83 mmol) and methanol (1 mL) were used. This composition corresponds to typical molar ratio of methanol to glyceryl triacetate equal to 29 which was commonly used in most research.[2] Toluene (30 mg, internal standard) and catalyst (30 mg) were separately added to the reactor as well. The mixture was heated at 50 °C for 3 hours and the reaction was quenched by ice-water bath. The quantification of the products was performed using GC calibrated for each compound with toluene as internal standard. GC-MS was used for identification of the products.

2.5 Transesterification of glyceryl tributyrate with methanol

Glyceryl tributyrate (302 mg, 1 mmol) and methanol (1.2 mL) were used. This composition corresponds to typical molar ratio of methanol to glyceryl tributyrate equal to 29. Toluene (40 mg, internal standard) and catalyst (30 mg) were separately added to the reactor as well. The mixture was heated at 60 °C for 4 hours and the reaction was quenched by ice-water bath. The quantification of the products followed the same methods as described above.

2.6 Reusability of catalyst

The reusability of IRMOF-10-ED was tested for transesterification of glyceryl triacetate with methanol. Glyceryl triacetate (905 mg), methanol (5 mL), and catalyst (50 mg) were used. Each time, the mixture was heated at 50 °C for 4 hours and quenched by ice-water bath. The reaction mixture was filtered; the mother liquor was analysized by GC and GC-MS, while the insoluble catalyst was washed with anhydrous methanol, dried at 80 °C for 6 hours under the vacuum, and reused directly as catalyst for the next run under the same conditions (Figure 6).

3 Results and Discussion

3.1 Amine-Functionalized MOFs

As IRMOF series,[10] both MOF-5 (referred to IRMOF-1 as well)[11] and IRMOF-10[12] were selected for dative PSM. IRMOF-10 shares the same cubic topology of the framework with its parent structure MOF-5, but replaces the connecting organic linker of 1,4-benzenedicarboxylic acidic (BDC) for MOF-5 with a 4,4′-biphenyldicarboxylic acid (BPDC).[10–12] Therefore, the structure of IRMOF-10 is similar to that of MOF-5 but is dramatically larger. MOF-5 has acidic properties and can act as a solid acid catalyst due to the existence of some defects.[13,14] The presence of structural defects in MOFs leads to the the formation of coordinatively unsaturated sites (CUS) which can be datively modified by organic ligands as reported by many literatures.[15] As illustrated in Scheme 1b, when one amine group of ethylenediamine (ED) is linked to the coordinatively unsaturated sites of Zn(II) in MOF-5, the other pendant amine group can play a role of immobilized base catalyst. Diamines such as ED and 4-dimethylaminopyridine (DMAP) were selected for dative PSM of MOFs to afford a solid base. In a typical procedure, the synthesis of ED-functionalized MOF-5 (MOF-5-ED) was performed in toluene under reflux conditions by coordination of ED to the CUS of MOF-5. Figure 1 shows the proposed structures of MOF-5-ED and IRMOF-10-ED.

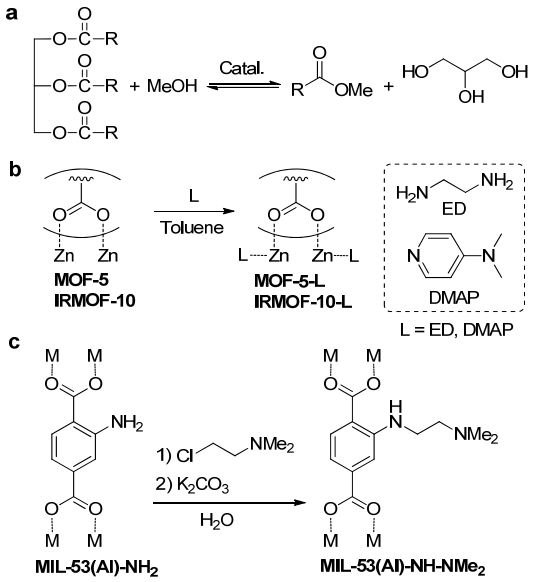

Scheme 1. (a) transesterification of triglycerides with methanol, (b) dative PSM on the SBUs of MOFs with ED and DMAP, (c) covalent PSM on the amine-tagged MOFs with aminoalkyl chloride.

The proofs of amine grafting were revealed by FT-IR, X-ray diffraction (XRD), ^{1}H NMR, nitrogen physisorption analysis, thermogravimetric analysis (TGA) and X-ray photoelectron spectroscopy (XPS). The FT-IR spectra of bare MOF-5 compound were compared with the two samples after ED- and DMAP-grafting (Figure S1). The peaks at 2980 and 2884 cm^{-1} assigned to ν(N-H) and ν(C-H) stretching vibrations, respectively, reveal the presence of ED in MOF-5-ED,[16] whereas the ν(C-N) stretching vibration at 1229 cm^{-1} indicates the presence of DMAP in MOF-5-DMAP.[17] Notably, the observed aliphatic C–H and N–H stretching vibrations in MOF-5-ED are upward shifted, compared with free ligand ED of 2926 and 2864 cm^{-1}.[18] The almost unchanged X-ray diffraction patterns show that the ED and DMAP grafting occur without apparent loss of crystallinity of MOF-5 with, however, some variation of the Bragg intensities (Figure 2), further indicating the successful functionalization of

MOF-5 with ED and DMAP.

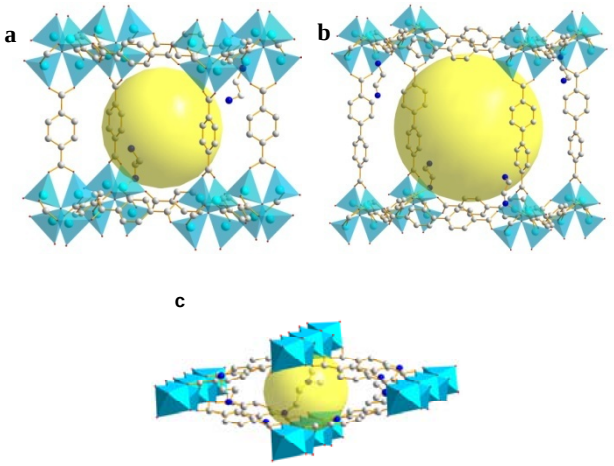

Figure 1. The proposed structures of (a) MOF-5-ED, (b) IRMOF-10-ED, (c) MIL-53(Al)-NH-NMe_2.

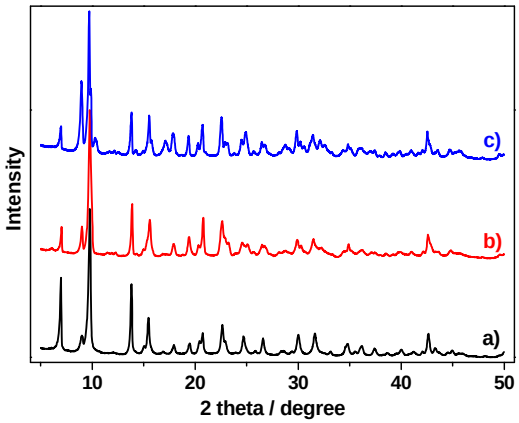

Figure 2. The XRD patterns of (a) MOF-5, (b) MOF-5-ED and (c) MOF-5-DMAP.

The ^{1}H NMR spectra of the digested ED- and DMAP-functionalized MOFs in DCl/D_2O/DMSO-d_6 provided further insights to precise amine loading levels. ^{1}H NMR of IRMOF-10-DMAP comprised only resonances attributable to BPDC and DMAP in a molar ratio of 3:3.8 (Figure 3d), producing an empirical formula of $Zn_4O(C_{14}H_8O_4)_3\cdot(DMAP)_{3.8}$. The Zn:DMAP stoichiometry of IRMOF-10-DMAP was thus accessible up to the maximum of four DMAP per empirical unit equivalent to one DMAP per Zn, suggesting a dative grafting rate of ~95% (based on metallic sites Zn). In the case of MOF-5-DMAP, the ^{1}H NMR integration provided a BDC:DMAP ratio of only 3:1.9 and thus produced an empirical formula $Zn_4O(C_8H_4O_4)_3\cdot(DMF)_{1.2}\cdot(DMAP)_{1.9}$ (Figure 3c). The DMAP was grafted to coordinatively unsaturated sites (Zn^{2+}) of MOF-5 and a relatively low DMAP-grafting rate of ~48% (based on metallic sites Zn) are presumably due to the fact that precursor MOF-5 processes relatively smaller pore size of 1.20 nm[12a] in contrast to 1.50 nm for IRMOF-10[12e] and therefore can only accommodate relatively few DMAP ligands in the MOF-5 cages.

Compared with the bare MOF-5, the resulting pore modification is also visible on the N_2 adsorption isotherms of the amine-functionalized MOF-5. Both MOF-5-ED and MOF-5-DMAP exhibit a significant decrease of porous surface area from 872 m^2g^{-1} for MOF-5[12a] to 391 m^2g^{-1} for MOF-5-ED and to 348 m^2g^{-1} for MOF-5-DMAP due to pore blocking, suggesting that both the ED and DMAP ligands are sufficiently bulky to crowd the pores of MOF-5 after ligand was grafted (Figure S2 and Table S1). In addition, the grafted amine groups are presumably present mainly at the defects of mesopore cages of MOF-5 because the defect centers provide the coordinatively unsaturated Zn^{2+} for ED and DMAP grafting.[15] Similar results are also observed in ED- and DMAP-functionalized IRMOF-10 (Figure S2 and Table S1).

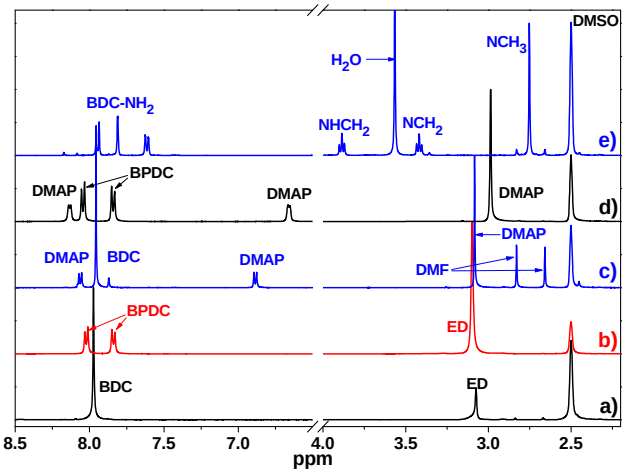

Figure 3. ^{1}H NMR spectra of digested (a) MOF-5-ED, (b) IRMOF-10-ED, (c) MOF-5-DMAP, (d) IRMOF-10-DMAP, and (e) MIL-53(Al)-NH-NMe_2 in a mixture of DCl/D_2O and DMSO-d_6.

The TGA data show that the ED- and DMAP-functionalized MOF-5 are stable at a temperature higher than the boiling point of the corresponding diamine, thus proving that the diamine was successfully anchored on the bare MOF-5 compound (Figure S3 and Table 1). The TGA of MOF-5-DMAP revealed mass losses of 8% at about 320 °C and 21% at 510 °C, assigned to coordinated DMF and DMAP, respectively. These results are in accordance with the empirical formula of MOF-5-DMAP provided by ^{1}H NMR analysis. In addition, MOF-5-DMAP shows a high thermostability up to 275 °C in contrast to MOF-5-ED at 200 °C, due to a stronger Zn-DMAP coordinate bond (Table 1).

IRMOF-10 and IRMOF-10-ED were evaluated further by XPS. The existence of an N 1s signal originating from IRMOF-10-ED further verifies the presence of ED in the IRMOF-10-ED (Figure S4a). The N 1s line of IRMOF-10-ED was deconvoluted into two superimposed peaks at 399.9 eV and 401.2 eV. The peak at 399.9 eV are characteristic peaks for the free amine group; whereas the peak at 401.2 eV are related to the coordinated amine group (Figure S4b).[19a] The XPS spectrum of Zn 2p in IRMOF-10 (Figure 4) can be deconvolved into doublet peaks with the

Cite this: DOI: 10.1039/c0xx00000x

www.rsc.org/xxxxxx

ARTICLE TYPE

Table 1. Properties of the amine-functionalized MOFs

Sample	Empirical formula[a]	TGA stability °C	Basic site density ($mmol \cdot g^{-1}$)	pH	Amine bp (°C)	pK_a[b] (amine)
MOF-5-ED	$Zn_4O(BDC)_3 \cdot (ED)_{1.2}$	up to 200	0.76	9.23	117-119	9.98
IRMOF-10-ED	$Zn_4O(BPDC)_3 \cdot (ED)_{4.2}$	up to 200	0.81	9.16	117-119	9.98
MOF-5-DMAP	$Zn_4O(BDC)_3 \cdot (DMF)_{1.2} \cdot (DMAP)_{1.9}$	up to 275	0.53	8.17	162 (50 mmHg)	9.20
IRMOF-10-DMAP	$Zn_4O(BPDC)_3 \cdot (DMAP)_{3.8}$	up to 315	0.59	8.21	162 (50 mmHg)	9.20
MIL-53(Al)-NH-NMe_2	$Al(OH)[(BDC\text{-}NH_2)_{0.55} \cdot (BDC\text{-}NHC_2H_4NMe_2)_{0.45}]$	up to 450	0.65	8.49	36-38 [c]	9.99 [c]

[a] based on ^1H NMR integration of digested MOFs in DCl/D_2O and DMSO-d_6 (Figure 3). [b] referred to 1) JR. H. K. Hall, J. Am. Chem. Soc., 1957, 79, 5441–5444; 2) D. R. Lide, CRC Handbook of Chemistry and Physics, CRC Press, London, 2001, 82. [c] *N*,*N*-dimethylethylamine (Me_2NEt) was referenced instead.

binding energy at 1019.3 eV (assigned to Zn $2p_{3/2}$) and 1042.2 eV (assigned to Zn $2p_{1/2}$), indicating the presence of the coordination of ligand BPDC with Zn.[19b,c] In the case of IRMOF-10-ED, the XPS spectrum of Zn can be deconvolved into two main doublet peaks (Figure 4). The characteristic peaks corresponding to framework groups of zinc carboxylate of IRMOF-10 are perfectly visible at 1019.3 eV and 1042.2 eV for IRMOF-10-ED. In addition, another new doublet peaks at 1020.8 eV and 1043.2 eV are related to the amine coordinated zinc.[19d,e] The above XPS spectra analysis thus confirmed the coordination of the ED with Zn within the IRMOF-10-ED.

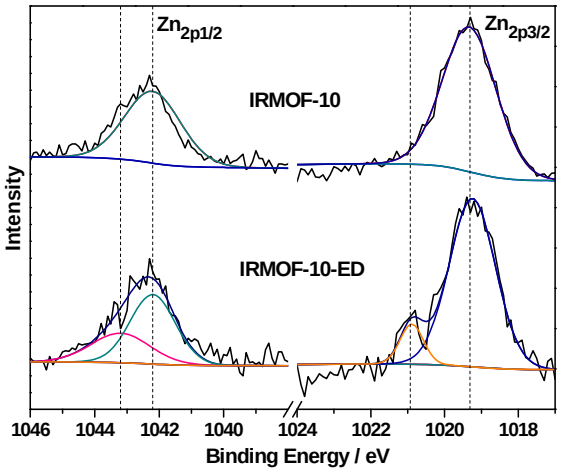

Figure 4. Zn 2p XPS spectra of IRMOF-10 and IRMOF-10-ED.

Besides dative PSM of MOFs, covalent PSM of the amine-tagged organic linkers within the framework of MIL-53(Al)-NH_2[20] was also achieved to produce solid base. As illustrated in Scheme 1c, alkylation of the aromatic amine tags (2-amino-1,4-benzenedicarboxylate, BDC-NH_2) in MIL-53(Al)-NH_2 with 2-dimethylaminoethyl chloride can produce new pendant aliphatic amine groups which, in principle, should be more basic than the pristine aromatic amines in MIL-53(Al)-NH_2. These pendant amine groups in MIL-53(Al)-NH_2 can play a role of immobilized base catalyst as well. Due to the fact that MIL-53(Al)-NH_2 possesses high thermal (up to 450 °C) and chemical stability to water and common organic solvents,[20] water was selected for reaction media. In a typical procedure of covalent PSM on the amine-tagged MOFs, a suspension of MIL-53(Al)-NH_2 in water is treated with 2-dimethylaminoethyl chloride with potassium carbonate as inorganic base to provide MIL-53(Al)-NH-NMe_2.

The covalent product MIL-53(Al)-NH-NMe_2 was characterized by XRD (Figure S5) and liquid ^1H NMR on a quantitative manner as well. After the covalent PSM of MIL-53(Al)-NH_2, there was no significant loss of crystallinity in X-ray diffraction patterns as shown in Figure S5, suggesting that the integrity of the MIL-53(Al)-NH_2 framework was maintained. Moreover, ^1H NMR spectra of the digested MIL-53(Al)-NH-NMe_2 (Figure 3e) comprised only resonances attributable to BDC-NH_2 moiety and *N*,*N*-dimethylaminoethyl group in the molar ratio of 1:0.45, indicating a covalent grafting rate of ~45% (based on organic linker BDC-NH_2) for MIL-53(Al)-NH_2.

Table 1 shows a comparison of the prepared amine-functionalized MOFs. The precise amine loading levels were determined by a solution ^1H NMR spectroscopy, whereas thermal stability was analyzed by TGA. The TGA of amine-functionalized MOFs further revealed that the amine-functionalized MOFs prepared by covalent PSM show a higher thermostability than in the case of dative PSM. The basicity properties and the number of accessible basic sites (basic site density) were characterized by potentiometric acid–base titration with HCl as the titrant. The apparent pH value was generated by suspending the corresponding MOFs in an aqueous solution. As described in Table 1, the basicity of the amine-functionalized MOFs was, in principal, determined by amine loading levels relative to bare MOFs and pK_a of the amine used; the basic site density of amine-functionalized MOFs decreases with the order of IRMOF-10-ED > MOF-5-ED > MIL-53(Al)-NH-NMe_2 > IRMOF-10-DMAP > MOF-5-DMAP.

3.2 Transesterification of Triglycerides

Recently, the transesterification of vegetable oil was reported by Chizallet and co-workers with non-functionalized MOFs (ZIF-8) as catalyst.[9a] Moreover, Farrusseng and co-workers recently reported transesterification of ethyldecanoate with MeOH using a bifunctional MOF catalyst[9b] and methanolysis of phenyl acetate by using pyridine-functionalized MOFs[9c]. Herein, the prepared amine-functionalized MOFs were tested as potential basic

heterogeneous catalyst. Their catalytic activity was evaluated for the transesterification of glyceryl triacetate and glyceryl tributyrate with methanol, respectively, which are considered as important model reactions for biodiesel production.[1–2] Initially, blank experiments of glyceryl triacetate methanolysis were carried out in the presence of bare MOFs to check the contribution from unfunctionalized MOFs. The conversions of glyceryl triacetate obtained in blank runs were remarkably inferior, ranging from 3.9 to 10.4% (Table 2, Entries 1–3). The observed catalytic performance of the unfunctionalized MOFs can presumably be related to Lewis acidity of unsaturated metallic sites in the bare MOFs upon removal of the terminal molecules such as water and DMF.

Table 2. The transesterification reactions over various amine-functionalized MOF catalysts

Entry	Catalyst	R	Time [h]	Conversion [%]
1[a]	IRMOF-10	Me	4	10.4
2	MOF-5	Me	4	9.2
3	MIL-53(Al)-NH_2	Me	4	3.9
4	IRMOF-10-ED	Me	3	>99.9
5	MOF-5-ED	Me	3	>99.9
6	MIL-53(Al)-NH-NMe_2	Me	4	>99.9
7	IRMOF-10-DMAP	Me	4	93.3
8	MOF-5-DMAP	Me	4	92.0
9[b]	IRMOF-10-ED	^{n}Pr	6	>99.9
10	MOF-5-ED	^{n}Pr	6	>99.9
11	MIL-53(Al)-NH-NMe_2	^{n}Pr	6	94.7
12	IRMOF-10-DMAP	^{n}Pr	6	83.9
13	MOF-5-DMAP	^{n}Pr	6	78.1

Conditions: [a] Catal. (30 mg), glyceryl triacetate (181 mg), methanol (1 mL), 50 °C (Entries 1–8). [b] Catal. (30 mg), glyceryl tributyrate (302 mg), methanol (1.2 mL), 60 °C (Entries 9–13).

Table 2 shows all of the amine-functionalized MOFs readily processed the transesterification of glyceryl triacetate and methanol (Scheme 1a) with excellent conversions from >99.9 to 92.0% at 50 °C (Entries 4–8), which is far higher than those achieved with regards to their corresponding bare precursors. In addition, these amine-functionalized MOFs also showed excellent to good catalytic performance towards transesterification of glyceryl tributyrate and methanol with glyceryl tributyrate conversions ranging from >99.9 to 78.1% (Table 2, Entries 9–13). Moreover, the methanolysis of glyceryl triacetate, short-chain triglyceride, with amine-functionalized MOFs as catalyst, shows relatively high yields than that of glyceryl tributyrate comprising relative long-chain triglycerides. By comparison, Figure 5b further shows that the turnover frequency (TOF) of glyceryl tributyrate methanolysis was only a half than in the case of glyceryl triacetate under the same condition as described in Figure 5a. The above results obtained with glyceryl triacetate indicate that the reaction presumably proceeds in the porous framework, whereas the accessibility of bulkier glyceryl tributyrate to the active sites in the pores of MOF catalyst is more difficult than in the case of glyceryl triacetate owing to the molecular sieving property of the MOFs.[9,21] This may result in less effective utilization of active sites in solid base MOF catalyst during transesterification.

Figure 5a shows the catalytic activity of amine-functionalized MOFs in the transesterification of glyceryl tributyrate and methanol decreases with the following order IRMOF-10-ED > MOF-5-ED > MIL-53(Al)-NH-NMe_2 > IRMOF-10-DMAP > MOF-5-DMAP. Notably, this result is in line with the sequence of basic site density for amine-functionalized MOFs as described in Table 1, suggesting that the solid base catalyst with the highest concentration of basic amine-groups proved to be the most active.

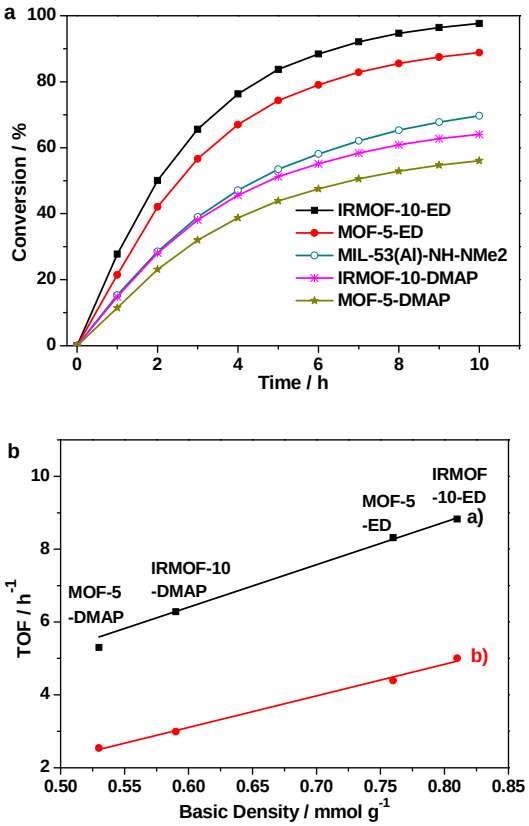

Figure 5. (a) The comparison of catalytic activities of amine-functionalized MOFs on the transesterification of glyceryl tributyrate and methanol (reaction conditions: glyceryl tributyrate, 2.100 g; methanol, 8.0 mL; catalyst, 80 mg; temperature, 60 °C); (b) linear correlations between basic density of amine-functionalized MOFs with their catalytic activity in the transesterification of a) glyceryl triacetate and b) glyceryl tributyrate with methanol, respectively.

Recent research suggested that the activity of solid base catalysts in transesterification is deeply influenced by basic sites on the catalyst surface.[1,2,22] However, the effects of solid base strength on catalytic activity in transesterification remains poorly understood. This is largely owing to the fact that the catalytic performances of these solid base catalysts and their corresponding morphology, basicity, surface structure, hydrophobicity, pore architecture are sensitive to their preparative methods. In our case, both of MOF-5 and IRMOF-10 have similar structure; moreover, the same PSM method of MOF-5 and IRMOF-10 makes the MOF-ED and MOF-DMAP ideal models to quantitatively investigate the relationship between the catalytic activity and basicity of MOF-catalyzed transesterification. Figure 5b further provides a deeper insight into the relationship between catalyst structure and performance, showing a linear correspondence between the catalytic activity in term of TOF and basic site density of amine-functionalized MOF catalysts in triglyceride transesterification.

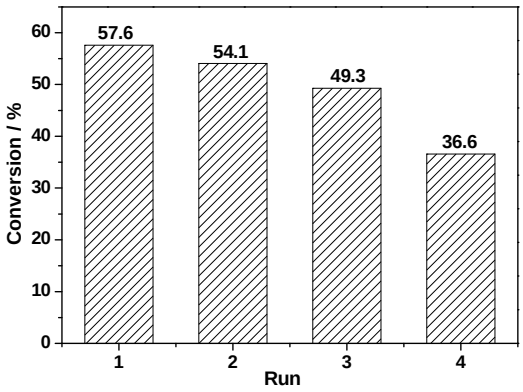

Figure 6. Catalyst recycling (reaction conditions: glyceryl triacetate, 905 mg; methanol, 5 mL; IRMOF-10-ED, 50 mg; temperature, 50 °C; time, 4 h).

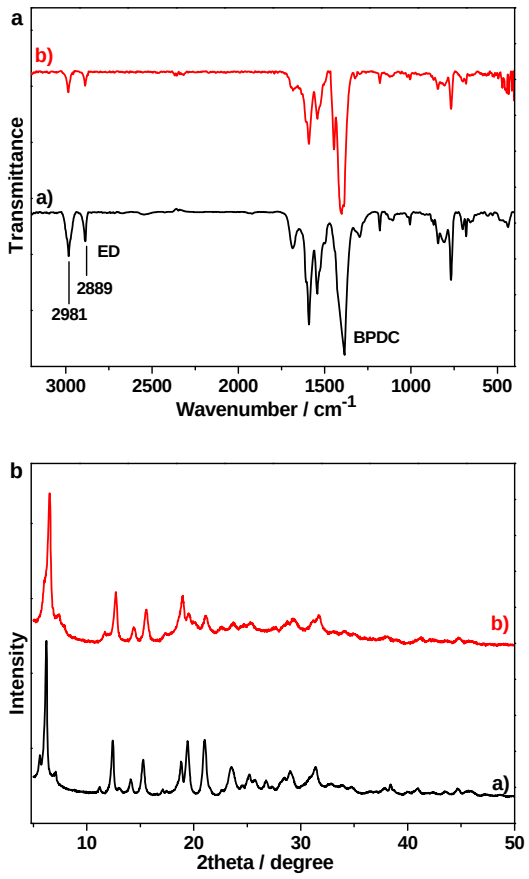

Figure 7. (a) FT-IR spectra and (b) XRD patterns of a) IRMOF-10-ED and b) recovered IRMOF-10-ED

The reusability of IRMOF-10-ED catalyst was tested for transesterification of glyceryl triacetate and methanol. The experiment was performed at a low glyceryl triacetate conversion level to obtain a further insight into the catalyst stability. The measured conversions of glyceryl triacetate decreased from 57.6 to 36.6% after a four-cycle experiment. This result indicates that IRMOF-10-ED partially lost their activity during the recycling process (Figure 6). Figure 7 shows FT-IR and XRD studies on a comparison between fresh and recovered catalysts. Notably, the relative intensity of ED to BPDC in the recovered IRMOF-10-ED significantly decreased than in the case of fresh one (Figure 7a). However, the XRD patterns of fresh and recovered IRMOF-10-ED are almost the same (Figure 7b). Therefore, the reduced activity of IRMOF-10-ED can presumably be related to the active species ED lost from IRMOF-10-ED during its recovery.

Figure 8a shows a typical transesterification reaction profile obtained using MOF-5-ED as catalyst. Glyceryl triacetate is quickly converted into methyl acetate and diglyceride. The further transesterification of the diglyceride to monoglyceride is initiated after 60 min. The yield of diglyceride has a maximum after 60 min. After this time the yield of diglyceride declines with the presence of monoglyceride. The influence of the reaction temperature on MOF-5-ED-catalyzed transesterification reaction revealed that increasing the reaction temperature generally leads to a promoted reaction (Figure 8b). The glyceryl triacetate was fully converted in 5 h at 50 °C, whereas it took 5 h to achieve a glyceryl triacetate conversion of 46% at 30 °C.

The molar ratio of the triglyceride to methanol is another important parameter in its transesterification owing to the fact that each step of transesterification reaction is reversible. A large excess of methanol is, in principle, required to shift the equilibrium to the product side. In our case, different glyceryl triacetate to methanol molar ratios (1:29, 1:20, 1:10, 1:5) were used, at a fixed temperature of 50 °C as well as a fixed amount of MOF-5-ED (Figure 8c). The transesterification system became more active as the amount of methanol increased. When using molar ratios of 1:29, a complete conversion was achieved in 5 h. With a ratio of 1:10, only 59% conversion was reached after 5 h; and in the case of the ratio 1:5, the conversion of glyceryl triacetate was remarkably inferior.

Kinetic studies of transesterification were carried out under optimum conditions with a molar ratio of methanol to glyceryl triacetate of 90:1 and IRMOF-10-ED as catalyst (Figure S6). Current research results show that the transesterification reaction obeys pseudo-first order reaction under the condition of high methanol-to-oil molar ratio.[23] The rate of transesterification (r[T]) can generally be expressed as the following equation:

$$-\mathrm{r[T]} = -\frac{d\mathrm{C[TG]}}{d\mathrm{t}} = \mathrm{kC[TG]}$$

where C[TG] and k are concentration of triglyceride and reaction rate constant.

$$\ln \mathrm{k} = -\frac{\mathrm{Ea}}{\mathrm{RT}} + \ln \mathrm{A}$$

According to the above Arrhenius equation, the original equation is transformed into the following equation with the C[TG] in terms of conversion X. Herein, t and C are the reaction time and an arbitrary constant, respectively.

$$-\ln(1-\mathrm{X}) = k\mathrm{t} + \mathrm{C}$$

After a data fitting as shown in Figure S6, the linear relationship between Ln (1-X) and reaction time (t) thus supported the hypothesis as pseudo-first order of the transesterification reaction

(Figure 9a). Based on the above Arrhenius equation, Figure 9b depicts the (Ln k) versus (1/T × 10^3), indicating that the activation energy (Ea) and pre-exponential factor (A) for the transesterification were 48.2 kJ mol^{-1} and 2.9 × 10^6 min^{-1}, respectively.

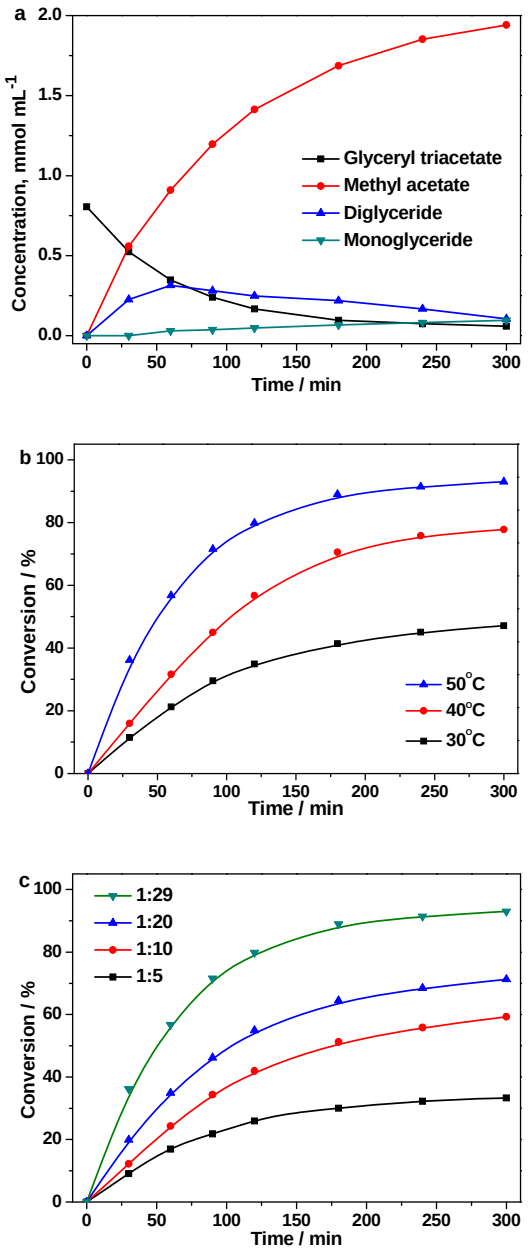

Figure 8. (a) Product distribution for MOF-5-ED catalyzed transesterification of glyceryl triacetate with methanol (reaction conditions: glyceryl triacetate, 181 mg; methanol, 1.2 mL; MOF-5-ED, 30 mg; temperature, 50 °C); (b) Influence of the reaction temperature on the transesterification of glyceryl triacetate with methanol (reaction conditions: glyceryl triacetate, 1.650 g; MOF-5-ED, 50 mg; methanol, 9.0 mL; temperature, 50, 40, and 30 °C, respectively); (c) Influence of the ratio of glyceryl triacetate to methanol on the transesterification of glyceryl triacetate (reaction conditions: glyceryl triacetate, 1.650 g; MOF-5-ED, 50 mg; methanol, 9.0, 6.2, 3.1, and 2.0 mL, respectively; temperature, 50 °C).

In addition, owing to the molecular sieving property of MOF-derived catalyst, it is very important to know whether the reaction is controlled by diffusion or kinetics. It is generally accepted that the diffusion limited reaction and kinetic limited reaction have as low as 10–15 kJ mol^{-1} and higher than 25 kJ mol^{-1} activation energies, respectively.[24] In our case, the activation energy of 48.2 kJ mol^{-1} obtained in this study thus demonstrated that the reaction rate is mainly controlled by kinetics. The above research provides a fundamental understanding towards transesterification of triglyceride with amine-functionalized MOF material as solid base catalyst.

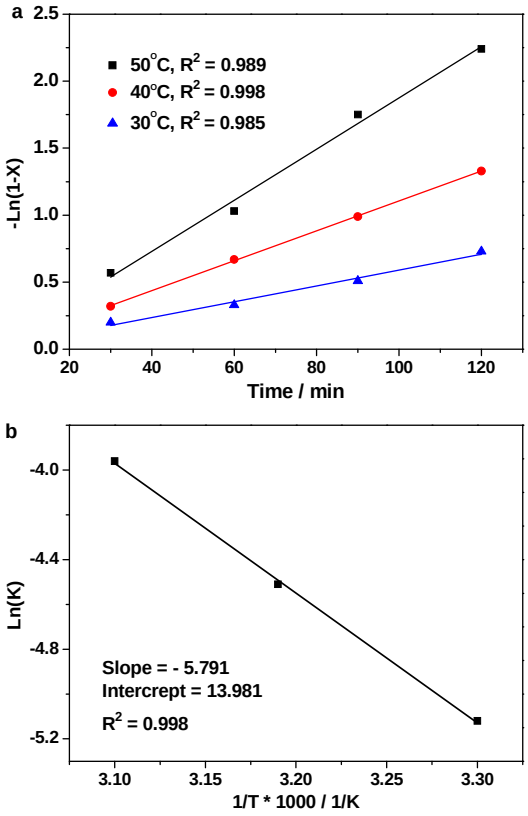

Figure 9. (a) The linear relationship between time and -Ln(1-X). (b) Ln k versus 1/T*1000 according to Arrhenius equation.

4. Conclusions

In conclusion, amine-functionalized MOFs, obtained from postsynthetic modification, show excellent performance as solid base catalysts towards the transesterification of triglycerides with methanol. The relationship between the catalytic activity and basicity of the amine-functionalized MOFs reveals a linear correspondence in terms of turnover frequency and the basic site density. The effects of mass transfer limitations on the transesterification reaction suggest that the reaction is partially mass transfer-dependent in the pore system of MOF catalysts. This research opens a new perspective on postsynthetic modification of MOFs and more generally on the rational design of MOF-derived solid base catalysts.

Acknowledgements

We are grateful for the financial support from National Natural Science Foundation of China (21172219 and 21207039), National Basic Research Program of China (973 Program, 2012CB215304), 100 Talents Program of the Chinese Academy of Sciences, and Guangdong Provincial Key Laboratory of Atmospheric Environment and Pollution Control.

Notes and references

[a] *CAS Key Laboratory of Renewable Energy, Guangzhou Institute of Energy Conversion, Chinese Academy of Sciences. Guangzhou 510640 (PR China). E-mail: chenjz@ms.giec.ac.cn. Tel./Fax: +86-20-3722-3380.*
[b] *Guangdong Provincial Key Laboratory of Atmospheric Environment and Pollution Control, College of Environment and Energy, South China University of Technology, Guangzhou 510006 (PR China)*
[c] *University of Chinese Academy of Sciences. Beijing 100049 (PR China).*

† Electronic Supplementary Information (ESI) available: [details of any supplementary information available should be included here]. See DOI: 10.1039/b000000x/

‡ Footnotes should appear here. These might include comments relevant to but not central to the matter under discussion, limited experimental and spectral data, and crystallographic data.

1 a) S. Lestari, P. Arvela, J. Beltramini, G. Q. Max Lu and D. Y. Murzin, *ChemSusChem*, 2009, **2**, 1109-1119; b) A. Sivasamy, K. Y. Cheah, P. Fornasiero, F. Kemausuor, S. Zinoviev and S. Miertus,. *ChemSusChem*, 2009, **2**, 278-300; c) K. Wilson, A. F. Lee, *Catal. Sci. Technol.* 2012, **2**, 884-897; d) M. Koberg, A. Gedanken, *Energy Environ. Sci.*, 2012, **5**, 7460-7469

2 a) D.-W. Lee, Y.-M. Park and K-Y Lee, *Catal. Surv. Asia*, 2009, **13**, 63-77. b) A. Zięba, A. Drelinkiewicz, E. N. Konyushenko and J. Stejskal, *Appl. Catal. A* 2010, **383**, 169-181; c) K. Narasimharao, D. R. Brown, A. F. Lee, A. D. Newman, P. F. Siril, S. J. Tavener and K. Wilson, *J. Catal.*, **248**, 226-234.

3 a) A. Villa, J.-P. Tessonnier, O. Majoulet, D. S. Su and R. Schlögl, *ChemSusChem*, 2010, **3**, 241-245; b) D. Farrusseng, C. Mirodatos, *Design of Heterogeneous Catalysts*, U. S. Ozkan, (Ed.), Wiley-VCH, 2009.

4 a) A. Corma, H. García and F. X. Llabrés i Xamena, *Chem. Rev.*, 2010, **110**, 4606-4655; b) S. M. Cohen. *Chem. Rev.*, 2012, **112**, 970-1000; c) K. K. Tanabe, S. M. Cohen, *Chem. Soc. Rev.*, 2011, **40**, 498-519; d) D. Zhao, D. J. Timmons, D. Q. Yuan and H-C. Zhou, *Acc. Chem. Res.*, 2011, **44**, 123-133; e) O. K. Farha and J. T. Hupp, *Acc. Chem. Res., 2010*, **43**, 1166-1175.

5 J. Z. Chen, S. P. Wang, J. Huang, L. M. Chen, L. L. Ma and X. Huang, *ChemSusChem*, 2013, **6**, 1545-1555.

6 a) M. O'Keeffe, O. M. Yaghi, *Chem. Rev.*, 2012, **112**, 675-702; b) S. Kitagawa, R. Kitaura and S.-I. Noro, *Angew. Chem. Int. Ed.*, 2004, **43**, 2334-2375.

7 a) J.-P. Zhang, Y.-B. Zhang, J.-B. Lin and X.-M. Chen, *Chem. Rev.*, 2012, **112**, 1001-1033; b) G. Aromí, L. A. Barrios, O. Roubeau and P. Gamez, *Coord. Chem. Rev.*, 2011, **255**, 485-546; c) C. R. Wade, T. Corrales-Sanchez, T. C. Narayan and M. Dincă, *Energy Environ. Sci.*, 2013, **6**, 2172-2177.

8 a) X.-J. Wang, P.-Z. Li, Y. Y. Chen, Q. Zhang, H. C. Zhang, X. X. Chan, R. Ganguly, Y. X. Li, J. W. Jiang and Y. L. Zhao, *Sci. Rep.*, 2013, **3**, 1149; b) S. Couck, Joeri F. M. Denayer, G. V. Baron, T. Rémy, J. Gascon and F. Kapteijn, *J. Am. Chem. Soc.*, 2009, **131**, 6326-6327; c) F. Wang, Y. X. Tan, H. Yang, Y. Kang and J. Zhang, J. *Chem. Commun.*, 2012, **48**, 4842-4844; d) L. F. Wang and R. T. Yang, *J. Phys. Chem. C.*, 2012, **116**, 1099-1106.

9 a) C. Chizallet, S. Lazare, D. Bazer-Bachi, F. Bonnier, V. Lecocq, E. Soyer, A-A. Quoineaud, and N. Bats, *J. Am. Chem. Soc.*, 2010, **132**, 12365-12377; b) M. Savonnet, A. Camarata, J. Canivet, D. Bazer-Bachi, N. Bats, V. Lecocq, C. Pinel and D. Farrusseng, *Dalton Trans.*, 2012, **41**, 3945-3948; c) M. Savonnet, S. Aguado, U. Ravon, D. Bazer-Bachi, V. Lecocq, N. Bats, C. Pinel and D. Farrusseng,. *Green Chem.*, 2009, **11**, 1729-1732.

10 M. Eddaoudi, J. Kim, N. Rosi, D. Vodak, J. Wachter, M. O'Keeffe and O. M. Yaghi, *Science*, 2002, **295**, 469-472.

11 a) L. M. Huang, H. T. Wang, J. X. Chen, Z. B. Wang, J. Y. Sun, D. Y. Zhao and Y. S. Yan, *Microporous Mesoporous Mater.*, 2003, **58**, 105-114; b) H. Furukawa, N. Ko, Y. B. Go, N. Aratani, S. B. Choi, E. Choi, A. Ö. Yazaydin, R. Q. Snurr, M. O'Keeffe, J. Kim and O. M. Yaghi, *Science*, 2010, **329**, 424-428.

12 a) S. X. Gao, N. Zhao, M. H. Shu and S. N. Che, *Appl. Catal. A* 2010, **388**, 196-201; b) R. C. Xiong, D. J. Keffer, M. Fuentes-Cabrera, D. M. Nicholson, A. Michalkova, T. Petrova, J. Leszczynski, K. Odbadrakh, B. L. Doss and J. P. Lewis, *Langmuir*, 2010, **26**, 5942-5950; c) L. Senesac, T. G. Thundat, *Mater. Today*, 2008, **11**, 28-36; d) T. A. Makal, A. A. Yakovenko and H.-C. Zhou, *J. Phys. Chem. Lett.*, 2011, **2**, 1682-1689; e) J. L. C. Rowsell and O. M. Yaghi, *J. Am. Chem. Soc.*, 2006, **128**, 1304-1315.

13 a) U. Ravon, M. Savonnet, S. Aguado, M. E. Domine, E. Janneau and D. Farrusseng, *Microporous Mesoporous Mater.*, 2010, **129**, 319-329; b) N. T. S. Phan, K. K. A. Le and T. D. Phan, *Appl. Catal. A* 2010, **382**, 246-253; c) J. Hafizovic, M. Bjørgen, U. Olsbye, P. D. C. Dietzel, S. Bordiga, C. Prestipino, C. Lamberti and K. P. Lillerud, *J. Am. Chem. Soc.*, 2007, **129**, 3612-3620; d) G. Calleja, J. A. Botas, M. G. Orcajo and M. Sánchez-Sánchez, *J. Porous Mater.*, 2010, **17**, 91-97.

14 F. X. Llabrés i Xamena, F. G. Cirujano and A. Corma, *Microporous Mesoporous Mater.*, 2012, **157**, 112-117.

15 a) A. Vimont, J-M. Goupil, J-C. Lavalley, M. Daturi, S. Surblé, C. Serre, F.Millange, G. Férey and N.Audebrand, *J. Am. Chem. Soc.*, 2006, **128**, 3218-3227; b) M. Dinca and J. R. Long, *J. Am. Chem. Soc.*, 2007, **129**, 11172-11176; c) C. Montoro, E. García, S. Calero, M. A. Pérez-Fernández, A. L. López, E. Barea and J. A. R. Navarro, *J. Mater. Chem.*, 2012, **22**, 10155-10158; d) S. Choi, T. Watanabe, T-H. Bae, D. S. Sholl and C. W. Jones, *J. Phys. Chem. Lett.*, 2012, **3**, 1136-1141.

16 a) D.-Y. Hong, Y. K. Hwang, C. Serre, G. Férey and J.-S. Chang, *Adv. Funct. Mater.*, 2009, **19**, 1537-1552; b) Y. K. Hwang, D-Y. Hong, J.-S. Chang, S. H. Jhung, Y.-K. Seo, J. Kim, A. Vimont, M. Daturi, C. Serre and G. Férey, *Angew. Chem. Int. Ed.*, 2008, **47**, 4144-4148.

17 a) M. J. Ingleson, R. Heck, J. A. Gould and M. J. Rosseinsky, *Inorg. Chem.*, 2009, **48**, 9986-9988; b) O. K. Farha, K. L. Mulfort and J. T. Hupp, *Inorg. Chem.*, 2008, **47**, 10223-10225.

18 a) K. Krishnan and R. A. Plane, *Inorg. Chem.*, 1966, **5**, 852-857; b) D. A. Young, T. B. F reedman, E. D. Lipp and L. A. Nafie, *J. Am. Chem. Soc.*, 1986, **108**, 7255-7263.

19 a) L. Y. Wu, H. J. Wang, H. C. Lan, H. J. Liu and J. H. Qu, *Sep. Purif. Technol.*, 2013, **117**, 118-123; b) L. S. Dake, D. R. Her and J. M. Zachara. *Surf. Interface Anal.*, 1989, **14**, 71-75; c) B. R. Strohmeier, *Surf. Sci. Spectra*, 1994, **3**, 128-134; d) S. A. Acharya, N. Maheshwari, L. Tatikondewar, A. Kshirsagar and S. K. Kulkarni, *Cryst. Growth Des.*, 2013, **13**, 1369-1376; e) S. Seifert, F. Simon, G. Baumann, M. Hietschold, A. Seifert and S. Spange, *Langmuir*, 2011, **27**, 14279-14289.

20 a) T. Ahnfeldt, D. Gunzelmann, T. Loiseau, D. Hirsemann, J. Senker, G. Férey and N. Stock, *Inorg. Chem.*, 2009, **48**, 3057-3604; b) J. Gascon, U. Aktay, M. D. Hernandez-Alonso, G. P. M. van Klink and F. Kapteijn, *J. Catal.*, 2009, **261**, 75-57; c) S. J. Garibay, Z. Wang and S. M. Cohen, *Inorg. Chem.*, 2010, **49**, 8086-8091.

21 J. S. Seo, D. Whang, H. Lee, S. I. Jun, J. Oh, Y. J. Jeon and K. Kim, *Nature*, 2000, **404**, 982-986.

22 J. M. Montero, P. Gai, K. Wilson and A. F. Lee, *Green Chem.*, 2009, **11**, 265-268.

23 a) A. Talebian-Kiakalaieh, N. A. S. Amin, A. Zarei and I. Noshadi, *Appl. Energy*, 2013, **102**, 283-292; b) A. Birla, B. Singh, S. N. Upadhyay and Y. C. Sharma, *Bioresour. Technol.*, 2012, **106**, 95-100.

24 G. C. Bond, Heterogeneous catalysis: principles and applications, Oxford chemistry series; 1974 Chapter 3, p 49.

Amine-functionalized Metal-Organic Frameworks are used as solid base for the transesterification of triglycerides with methanol.

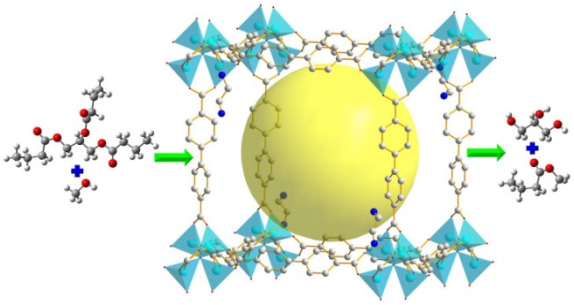

TOC